Available online at www.sciencedirect.com

SCIENCE DIRECT®

Remote Sensing of Environment 93 (2004) 198–210

Remote Sensing of Environment

www.elsevier.com/locate/rse

# Object-oriented image analysis for mapping shrub encroachment from 1937 to 2003 in southern New Mexico

Andrea S. Laliberte[a,*], Albert Rango[a], Kris M. Havstad[a], Jack F. Paris[b], Reldon F. Beck[c], Rob McNeely[c], Amalia L. Gonzalez[a]

[a]USDA-ARS Jornada Experimental Range, 2995 Knox St., Las Cruces, NM 88003, USA
[b]DigitalGlobe Inc., 1900 Pike Road, Longmont, CO 80501, USA
[c]Department of Animal and Range Sciences, New Mexico State University, Las Cruces, NM 88003, USA

Received 23 March 2004; received in revised form 16 July 2004; accepted 18 July 2004

**Abstract**

Shrub encroachment into arid and semi-arid grasslands in the southwestern United States is of concern because increased shrub cover leads to declines in species diversity, water availability, grazing capacity, and soil organic matter. Although it is well known that shrubs have increased over time, we have little quantitative information related to the non-linear nature of this vegetation change over a particular period. On the Jornada Experimental Range (JER; USDA-ARS) and the adjacent Chihuahuan Desert Rangeland Research Center (CDRRC; New Mexico State University) in southern New Mexico, shrub increase has been measured with various ground survey techniques extending back to 1858. For this study, we used 11 aerial photos taken between 1937 and 1996 that covered a 150-ha study area and had sufficient resolution for shrub detection. A QuickBird satellite image provided coverage for 2003. We used image segmentation and object-based classification to monitor vegetation changes over time. Shrub cover increased from 0.9% in 1937 to 13.1% in 2003, while grass cover declined from 18.5% to 1.9%. Vegetation dynamics reflected changes in precipitation patterns, in particular, effects of the 1951–1956 drought. Accuracy assessment showed that shrub and grass cover was underestimated due to the constraint of the pixel size. About 87% of all shrubs >2 $m^2$ were detected. The use of object-based classification has advantages over pixel based classification for the extraction of shrubs from panchromatic aerial and high-resolution satellite imagery. Incorporating both spectral and spatial image information approximates the way humans interpret information visually from aerial photos, but has the benefit of an automated classification routine. Combining several scales of analysis in a hierarchical segmentation method is appropriate in an ecological sense and allows for determining shrub density in coarser level classes. Despite encountering difficulties in analyzing a greatly varying aerial photo data set, including variability in spectral and spatial resolutions, moisture conditions, time of year of observation, and appearance of grass cover, aerial photos provide an invaluable historic record for monitoring shrub encroachment into a desert grassland.


*Keywords:* Object-based classification; Segmentation; Shrub encroachment; Desert grassland; Aerial photography; Satellite image

## 1. Introduction

Shrub encroachment into arid and semiarid grass-dominated landscapes has been noted in many parts of the Southwestern United States (Archer, 1994; Archer, 1995; Grover & Musick, 1990) and is of concern because shrub increase reduces species diversity and has a direct influence on changes in the water, carbon, and energy cycles of these arid lands (Schlesinger et al., 1990). In the Jornada basin of southern New Mexico, vegetation surveys date back as far as 1858 (Gibbens et al., in press). Researchers at two rangeland research field stations, the Jornada Experimental Range (JER; USDA-ARS; 783 $km^2$) established in 1912 and the adjacent Chihuahuan Desert Rangeland Research Center (CDRRC; New Mexico State University; 259 $km^2$) established in 1927, have used various ground survey techniques to track long-term shrub increases from 1858 to 1998

* Corresponding author. Tel.: +1 505 646 4144; fax: +1 505 646 5889.
*E-mail address:* alaliber@nmsu.edu (A.S. Laliberte).

0034-4257/$ - see front matter © 2004 Elsevier Inc. All rights reserved.
doi:10.1016/j.rse.2004.07.011

(Buffington & Herbel, 1965; Hennessy et al., 1983; Gibbens et al., in press).

Although remotely sensed data only date back to the 1930s (for aerial photography), they cover more extensive areas than single plot studies, and spatial patterns are easier to discern from photos than from the ground (Goslee et al., 2003; Rango et al., 2002). Remote sensing has been used in many areas of the world to track woody species encroachment (Brown & Carter, 1998; Hudak & Wessman, 1998; McCloy & Hall, 1991; Whiteman & Brown, 1998). At the Jornada Experimental Range, only one study examined shrub increase over time using high-resolution images (Goslee et al., 2003).

Image classifications derived from images with relatively large pixel sizes like 15–1000 m (MODIS, Landsat, AVHRR, etc.) are usually based on the spectral information contained in a single pixel. Smaller pixel sizes combined with fewer spectral bands in aerial photography and new high-resolution satellite imagery (IKONOS, QuickBird) can create classification problems due to greater spectral variation within a class and a greater degree of shadow. Simple thresholding can be applied to detect shrubs in panchromatic aerial photography (Hansen & Ostler, 2001), but this can result in many errors of commission and omission because shrubs may have the same reflectance as some background areas.

However, much information is contained in the relationship between adjacent pixels, including texture and shape information, which allows for identification of individual objects as opposed to single pixels (Thomas et al., 2003). Such an object-oriented approach allows the user to apply locally different strategies for analysis. Incorporating both spectral information (tone, color) as well as spatial arrangements (size, shape, texture, pattern, association with neighboring objects) comes closer to the way humans interpret information visually from aerial photos and has shown success in mapping shrubs (Hudak & Wessman, 1998) and detecting urban land use change (Herold et al., 2003). Franklin et al. (2000), for example, found that the incorporation of texture in addition to spectral information increased classification accuracy on the order of 10–15%.

Ecologically speaking, it is more appropriate to analyze objects as opposed to pixels because landscapes consist of patches that can be detected in the imagery with object-based analysis. Pixels are aggregated into image objects by segmentation, which is defined as the division of remotely sensed images into discrete regions or objects that are homogenous with regard to spatial or spectral characteristics (Ryherd & Woodcock, 1996). Homogenous in this case refers to the fact that the within-object variance is less than the between-object variance.

Image segmentation is appealing for remote sensing applications because human vision tends to generalize images into homogenous areas. Research into image segmentation is not new (Haralick et al., 1973) and several methods exist. They can be broadly categorized into measurement–space-guided spatial clustering, single-linkage region growing, spatial clustering, hybrid–linkage region growing, centroid–linkage region growing, and split-and-merge methods (Haralick & Shapiro, 1985), or more simply, into edge-based and area-based algorithms (Blaschke & Strobl, 2001). Reed and Wechsler (1990) used a filter-based approach to segment texture images, while Haddon and Boyce (1990) incorporated edge detection into their segmentation algorithm. Recent developments include a probability-based image segmentation approach (Abkar et al., 2000) and a fractal net evolution approach (FNEA), which is a multifractal approach (Baatz & Schaepe, 2000).

With the FNEA, images are segmented at different scales which adds a scale hierarchy to the analysis (Burnett & Blaschke, 2003; Hay et al., 2002). Such a multiresolution analysis using image segmentation is driven by remotely sensed data as well as expert knowledge, leading to a better understanding of the image content because image information is fractal in nature. This approach is also more appropriate ecologically because objects in a landscape are scale-dependent (Turner & Gardner, 1994). Unlike other segmentation approaches, such as watershed algorithms, region growing, or Markov random fields, the FNEA requires the user to determine certain scale-related parameters. A specific level of analysis produces objects at a certain scale (Blaschke & Hay, 2001). The network developed through classification and interdependencies of image objects and land use/land cover classes has been termed a spatial semantic network (Benz et al., 2004).

Our objective was to use aerial photos for measuring shrub and grass cover dynamics over a 66-year period in the Jornada Basin of southern New Mexico by combining multiresolution image segmentation and object-oriented image classification. A second objective was to compare the current shrub cover as measured from a 2003 QuickBird satellite image to ground measurements.

## 2. Methods

### 2.1. Study area

Our research was conducted on the CDRRC located approximately 28 km north of Las Cruces, New Mexico in the northern part of the Chihuahuan Desert (Fig. 1). The area is part of the Jornada Basin situated at about 1200 m elevation between the Rio Grande Valley in the west and the San Andres Mountains in the east. Average monthly maximum temperatures range from 13 °C in January to 36 °C in June, and mean annual precipitation is 241 mm of which more than 50% occurs in July, August, and September, although rainfall amount and distribution can be highly variable. Droughts, defined as years with <75% of mean annual precipitation occurred in 18 years between 1915 and 1995 (Havstad et al., 2000).

We selected a 150-ha area in pasture 2 for our analysis. Shrubby vegetation in the study area is comprised of honey mesquite [*Prosopis glandulosa* Torr.], broom snakeweed

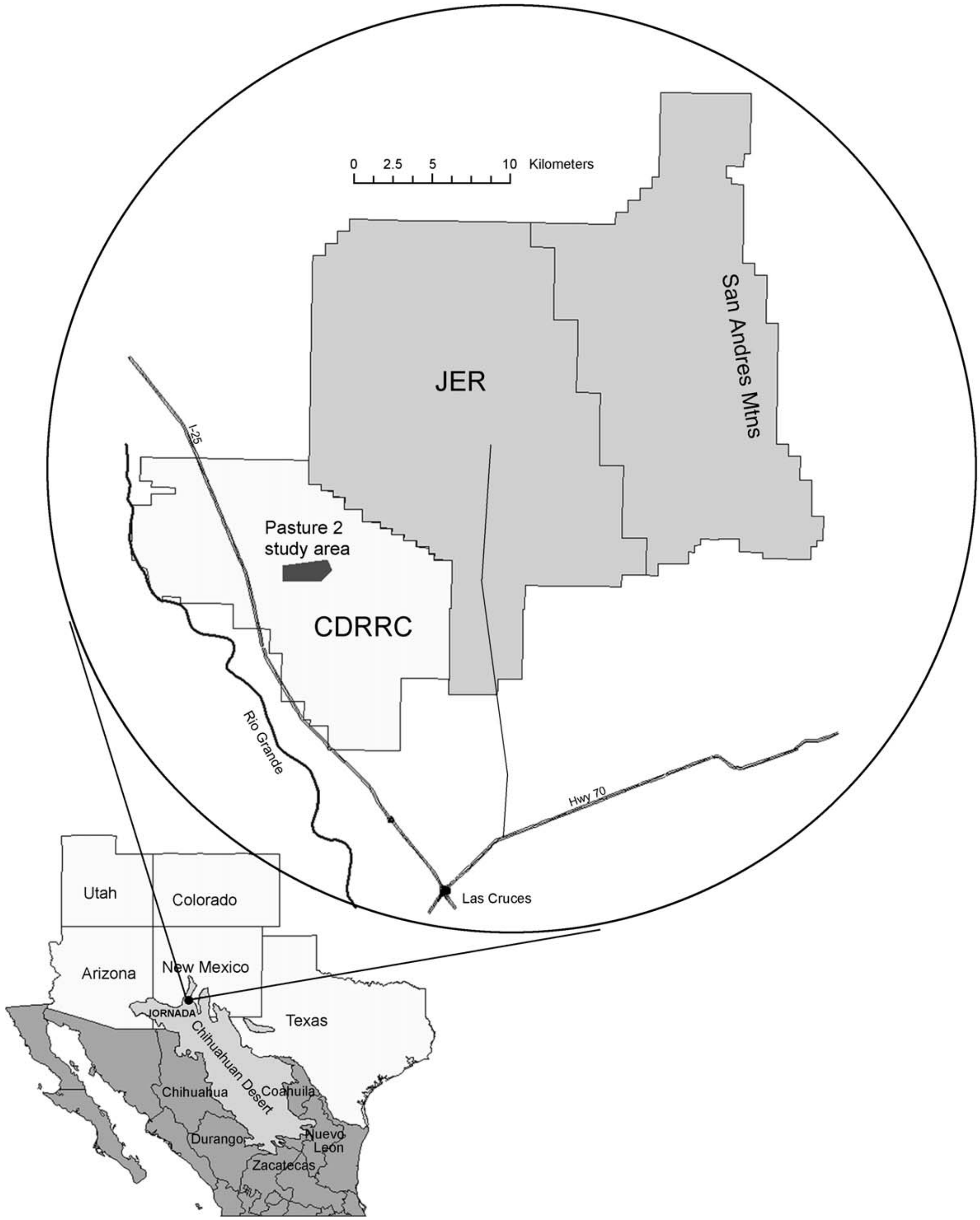


Fig. 1. Location of study area and rangeland research facilities in southern New Mexico.

[*Gutierrezia sarothrae*], creosote bush [*Larrea tridentata*], mormon tea [*Ephedra torreyana*], four-wing saltbush [*Atriplex canescens*], and soap-tree yucca [*Yucca elata*]. Grasses include black grama [*Bouteloua eriopoda*], tobosa [*Pleuraphis mutica*], dropseed species [*Sporobolus* spp.], and bush muhly [*Muhlenbergia porteri*].

Mesquite is the dominant species in the study area today, and historic records indicate that this species is the most aggressive invading shrub in the Jornada basin (Buffington & Herbel, 1965). Starting in the 1950s, herbicides were applied to many pastures on the CDRRC. Those treatments were effective in controlling the shrub advance if used on a regular basis. Record keeping was not consistent, and the widespread use of herbicides has made it difficult to assess how rapidly the shrubs were invading grassland areas in the last 60+ years. According to CDRRC records, pasture 2 was only treated with herbicides twice, in June 1973 and June 1984, and the treatment efficacy was relatively low.

### 2.2. Image analysis

Since 1936, 37 separate aerial photography missions have been flown over the Jornada Basin. Recently, the area has been imaged with high-resolution commercial satellites as well. We selected 11 aerial photos that covered the study area and had sufficient resolution for shrub detection. A QuickBird satellite image was used for the 2003 coverage of the area. For the aerial photography, we scanned the film with an Epson 1640 XL large-format flatbed scanner at 1200 dpi (dots per inch) in 8 bits for grayscale and 24 bits for color and color infrared film. The images were color balanced, imported into Erdas Imagine 8.6 and georectified to a digital orthoquad image of the area. All images were resampled with the nearest neighbor method to a common resolution of 86 cm (Table 1). Nearest neighbor resampling was used because it is computationally simple and does not alter original pixel values (Lillesand & Kiefer, 2000). All images were smoothed with a low-pass filter using a 3×3 kernel to reduce the spatial frequency. Such a slightly blurred image will produce a segmentation with fewer and more homogenous areas, so that shrubs are more likely to be represented by fewer polygons.

We chose to resample to a common resolution so that shrubs of interest would be either equal to or larger than the pixel size; a shrub would therefore represent a high resolution or H-res object (Hay et al., 2001; Woodcock & Strahler, 1987). If images were to be analyzed in their native resolution, shrub cover would presumably be somewhat higher in high resolution images because small shrubs could be resolved in high resolution but not in lower resolution images. Therefore, our approach does not represent shrub cover at the original image scale, but it allowed us to compare shrub cover at the chosen scale across time. Radiometric normalization of the images was not deemed necessary because the object-oriented image analysis approach relied on the differences between shrubs and background, not on absolute brightness values that could be compared across images.

We used the fractal net evolution approach (FNEA), which is an object-oriented multiscale image analysis method embedded in the software eCognition (Baatz & Schaepe, 2000; Definiens, 2003). The first step is a segmentation of the image based on three parameters: scale, color (spectral information), and shape (smoothness and compactness), where color and shape parameters can be weighted from 0 to 1. Within the shape setting, smoothness and compactness can also be weighted from 0 to 1. Scale is a unitless parameter related to the image resolution. Table 2 shows the images and the segmentation parameters used in this study. The segmentation used in eCognition is a bottom-up region merging technique, where the smallest object contains one pixel. In subsequent steps, smaller image objects are merged into larger ones based on the chosen scale, color, and shape parameters, which define the growth in heterogeneity between adjacent image objects. This process stops when the smallest growth exceeds the threshold defined by the scale parameter. A larger-scale parameter results in larger image objects (Benz et al., 2004).

This procedure produces highly homogeneous segments in a selectable resolution and of a comparable size. Classification is then performed using those objects rather than single pixels. The multiresolution segmentation approach allows for segmentation at different scales, which is used to construct a hierarchical network of image objects representing the image information in different spatial resolutions simultaneously. The image objects “know” their horizontal neighbors (adjacent objects on the same level) as well as their vertical neighbors (objects on different hierarchical levels); the latter are also termed sub-objects and super-objects. This allows for differentiation of individual shrubs on the lower level, and determination of different shrub density classes on a higher level.

The classification of the image objects can be performed by using nearest neighbor classifiers based on user-selected samples or by using membership functions, based on fuzzy logic theory combined with user-defined rules. A membership function ranges from 0 to 1 for each object’s feature values with regard to the object’s assigned class. The fuzzy rule base defines criteria such as “all image objects darker than a certain brightness value are shrubs”. Spectral, shape, and statistical characteristics as well as relationships between linked levels of the image objects can be used in the rule base to combine objects into meaningful classes (Benz et al., 2004).

The image analysis steps are described below and graphically in the flowchart (Fig. 2). We segmented the images at

Table 1
Images used in the analysis

| Year | Type | Resolution (m) |
|---|---|---|
| 1937 | Pan | 0.61 |
| 1947 | Pan | 0.23 |
| 1955 | Pan | 0.24 |
| 1960 | Pan | 0.43 |
| 1967 | Pan | 0.46 |
| 1973 | Pan | 0.78 |
| 1977 | CIR | 0.42 |
| 1980 | Color | 0.68 |
| 1989 | Color | 0.52 |
| 1991 | CIR | 0.59 |
| 1996 | CIR | 0.86 |
| 2003[a] | Pan | 0.60 |

Pan, panchromatic; CIR, color infrared.
[a] QuickBird satellite image.

Table 2
Segmentation parameters used for the analysis

| Segmentation level | Scale | Color | Shape | Shape settings | |
|---|---|---|---|---|---|
| | | | | Smoothness | Compactness |
| Level 1 | 3 | 0.8 | 0.2 | 0.8 | 0.2 |
| Level 2 | 250 | 0.8 | 0.2 | 0.5 | 0.5 |

Scale is a unitless parameter related to the image resolution. Values for color and shape as well as smoothness and compactness are weighting factors ranging from 0 to 1.

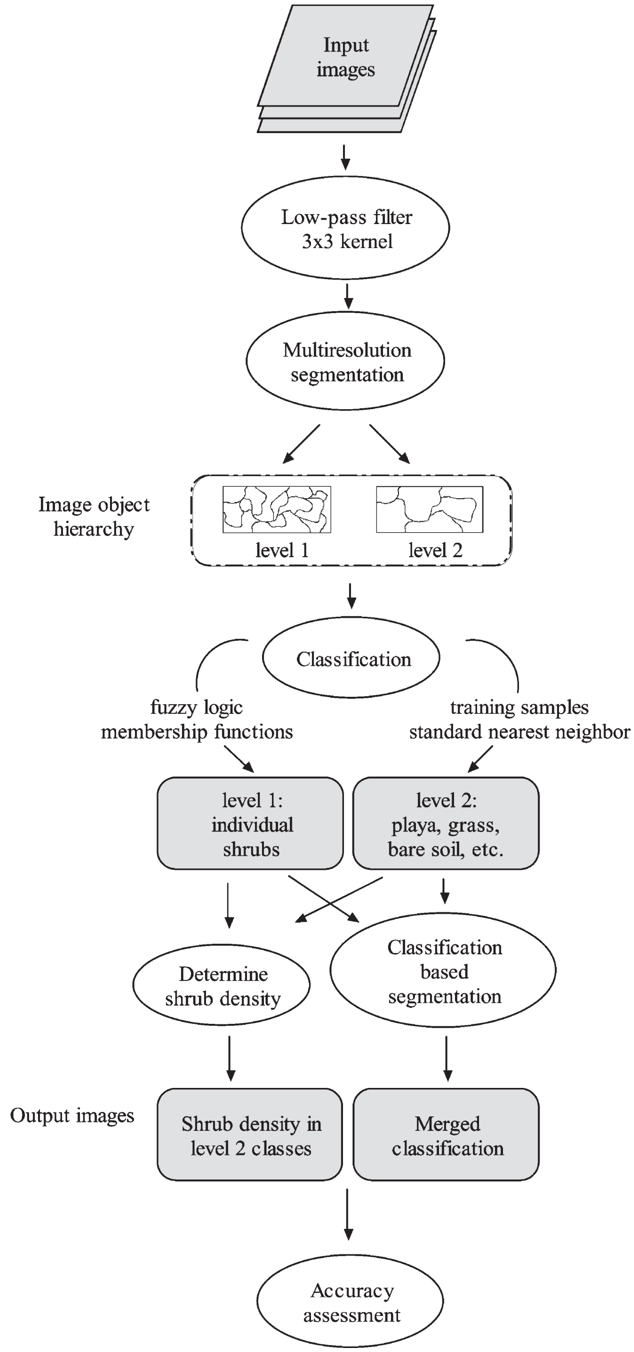


Fig. 2. Workflow of image analysis.

two scales of the image object hierarchy: a fine scale to capture single shrubs and a coarser scale to define broader landscape elements. Shrubs were then classified on the fine-scale level by defining the following membership functions:

(1) mean brightness value,
(2) mean difference to neighbors, and
(3) mean difference to super object.

If only membership function 1 is used, which is comparable to a thresholding procedure, large portions of dark background (occurrences of black grama) are classified as shrubs. Membership function 2 determines the layer mean difference for neighboring objects weighted with regard to the length of the border between objects. Membership function 3 determines the layer mean difference values between objects on the fine scale to objects at the coarser scale level. All three functions generate equal weight in the analysis and were combined by a logic "and" (minimum operator) function, which equals the minimum fulfillment of the single statements. Using this combination of membership functions is similar to how humans analyze an image and recognize shrubs in a dark background (shrubs occurring with black grama) as well as in a light background (against a bright soil background).

In addition to the shrub classification, we also performed a classification at the coarser level to determine how grass cover had changed over time. Because shrubs and grasses had similar brightness values in panchromatic imagery and could be confused with each other, a segmentation resulting in polygons larger than the largest shrub patch allowed for separation of grasses and shrubs. This classification was performed using a standard nearest neighbor classifier, with user-selected samples similar to a supervised classification in a pixel-based image analysis system. The image was classified into four classes: playa, bright soil, grass, and others. The samples (polygons) were selected by brightness values: bright soil represented the highest (brightest) values, grass the lowest (darkest) values, playa was a visible feature and all other polygons were placed in the 'others' class. This discrimination of classes was based on our knowledge that black grama in our study area had low reflectance values in aerial photos. Due to the limitations with historic images, we were only able to map distinct areas of black grama and bright soil; therefore, the 'others' class is relatively large.

By using information from both classification levels, we were then able to determine percent shrub cover in level 1 within the level 2 classes. Finally, a classification-based segmentation was performed. This is an advanced segmentation based on the previous classifications of both levels with the aim of creating a final classification. In this last step, the classified levels were merged to incorporate classes from both levels (shrub, grass, playa, bright soil, and others).

### 2.3. Ground truthing

It was assumed that the classification accuracy of the aerial photos was similar to the satellite image, which was the only one we could use for accuracy assessment. We randomly located twenty 400 $m^2$ plots in the pasture 2 study area to compare percent shrub cover from the classification of the 2003 QuickBird image with ground-based measurements. Field work was conducted on February 2004. We used a Trimble Pro XR® GPS unit to determine the plot corners and then traced the perimeter of each shrub that was larger than 50 cm in diameter in a walking survey. After differential correction, the area of each shrub was calculated. A previous experiment had shown a high correlation between shrub areas measured from GPS and shrub areas manually measured by taking the product of the longest axis of the shrub and the axis perpendicular to it ($n$=61, $P$=0.0019, $R^2$=0.9891; data not shown). In addition to comparing shrub areas in the plots, we also determined the size of shrubs that could be detected and classified with the QuickBird image. Due to the small amount of grass cover in the study area, we were able to determine total grass cover with GPS measurements as well and compare this with grass cover from the classification.

## 3. Results

### 3.1. Vegetation change

Shrub cover increased from 0.9% in 1937 to 13.1% in 2003 in pasture 2 (Fig. 3). The greatest increase occurred between 1937 and 1947 (38% increase). In 1960, shrub cover increased to 10.9%, decreased in 1967, then fluctuated around 8% before resuming an increase from 1991 to 2003 (Fig. 4).

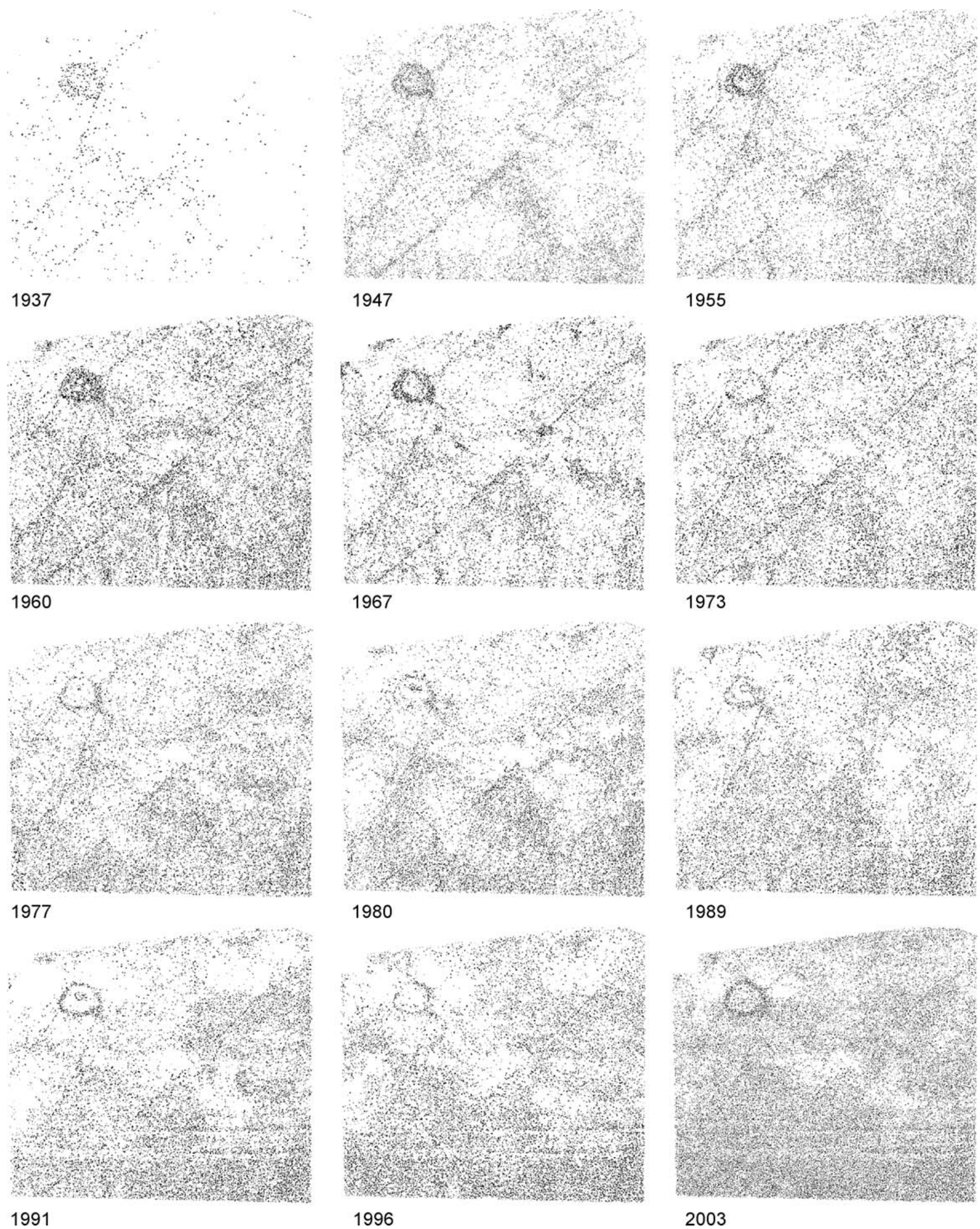


Fig. 3. Shrub cover change from 1937 to 2003, based on results from an object-based classification of the images on level 1 of the image object hierarchy.

The high shrub cover in 1960 may be partially attributed to image quality. Although all images were resampled to the same pixel size, shrubs appeared larger and separate shrubs tended to merge in the 1960 image. Although shrubs appeared to be less defined in the 2003 QuickBird image compared to the aerial photos, visual inspection confirmed that a larger proportion of small shrubs were captured. This was related to the greater bit depth of the QuickBird image.

The objective of the classification at level 2 of the image object hierarchy was to determine changes in grass cover over time (Fig. 5). Grass cover decreased from 18.5% in 1937 to 1.9% in 2003 (Fig. 4). As shrub cover increased, grass cover decreased over time. This is especially noticeable from 1937 to 1960, and again after 1996. The high value for grass cover in the image taken on October 8 1996 is related to a higher than average precipitation for September. Data for six rain gauges located within a 6-km radius of the study area indicated that the September precipitation was on average 72% higher (range, 33–99%) than the long-term rainfall data (1937–2003) for the same month (Table 3).

We calculated the percent shrub cover within the four classes of the level 2 classification. Percent shrub cover within three classes (grass, bright soil, and others) followed the same trend until 1955, then diverged with higher shrub cover in the grass compared to the bright soil and others classes (Fig. 6). After 1989, the shrub cover in these classes was similar. The playa showed a peak for percent shrub cover in 1967, then decreased and fluctuated similar to shrub cover in the other three classes. Sometime after 1967, mesquite plants in the playa were removed while improving a watering tank for livestock. The peak for the grass and others classes in 1960 should be treated with caution due to the image quality discussed above.

### 3.2. Object-oriented image analysis for shrub detection

The use of object-oriented image analysis proved to be advantageous in this study. Shrubs were present in both dark and light backgrounds, which could have presented a problem using a pixel based analysis. Fig. 7(a) shows a portion of the original QuickBird image that was segmented at a lower level (b) and at a higher level (c) of the image object hierarchy. A classification using only the mean spectral reflectance of the segmented objects (similar to a pixel based classification) at level 1 resulted in an overestimation of shrubs in the playa due to similar spectral properties of shrubs and portions of the background as well as many missed shrubs in other areas (d). Incorporating the linkage between neighboring objects and different levels allowed for differentiating shrubs in the dark background of the circular playa by including two additional membership functions: the mean difference to the super-object and the mean difference to neighbors. This resulted in an improved classification of shrubs (e). The final step was to perform a classification-based segmentation to combine the classifications of levels 1 and 2 in a final merged classification (f).

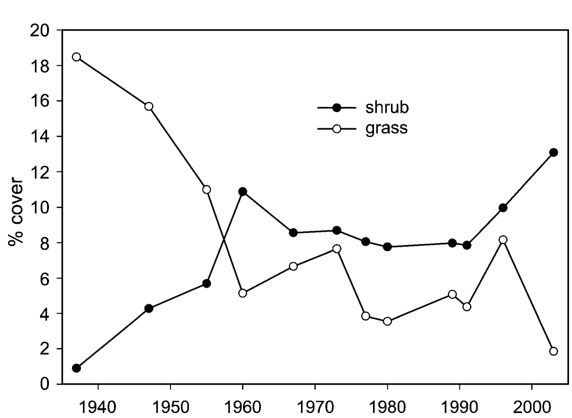


Fig. 4. Dynamics of shrub (●) and grass (○) cover from 1937 to 2003. Results are based on the merged classification of levels 1 and 2 of the image object hierarchy.

### 3.3. Accuracy assessment

The mean shrub area for the 20 ground truthing plots (400 $m^2$) was 82.7 $m^2$ for the GPS measurements compared to 61.5 $m^2$ for the image classification ($P$=0.008). It was expected that the classification would underestimate the actual shrub cover on the ground for two reasons. First, shrubs are outlined exactly with GPS, but are gross generalizations in a classification, which depicts shrubs as multiple blocks of pixels. The outer perimeter of a shrub contains lighter pixels than the interior, and because we traced shrub perimeters at the furthest most branches from the shrub center, areas of lighter pixels were often missed at the edges of shrubs. Therefore, many classified shrubs were smaller than the GPS outlines. Secondly, we included every shrub >50 cm in diameter in the GPS measurements, and many small shrubs were not detected in the classification. Small shrubs were included in the ground survey to determine a cutoff size at which shrubs could actually be classified. The size distribution for the shrubs showed that shrubs not detected by the classification had a mean area of 1.6 $m^2$ compared to 8.4 $m^2$ for detected shrubs (Table 4). About 87% of all shrubs larger than 2 $m^2$ were detected.

The area of grass from the classification was 2.2 ha compared to 2.6 ha from the GPS ground truthing. There were errors of commission and errors of omission, and as with the shrubs, grass areas were underestimated due to the exact outline of the GPS method compared with the more blocky classification. We assumed that the accuracy for aerial photos would be similar to the one obtained from the QuickBird image because all analyses were done on the panchromatic band and all images were resampled to the same resolution.

## 4. Discussion

In this pasture 2 study area, the average rate of increase of shrub cover percentage was about 0.2% per year over the

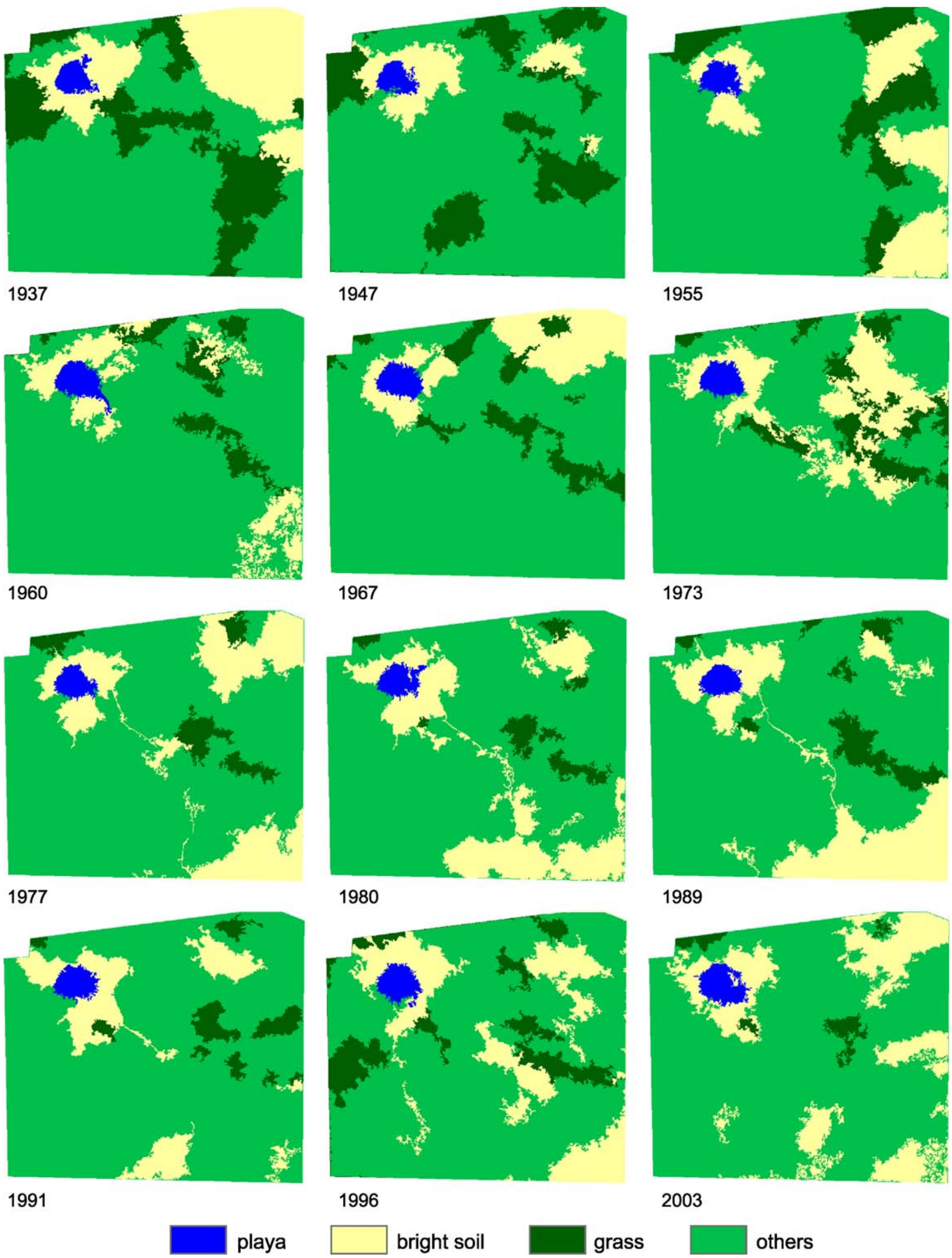


Fig. 5. Changes in land cover classes from 1937 to 2003, based on results from an object-based classification of the images on level 2 of the image object hierarchy.

66-year period. However, most of the shrub increase occurred between 1937 and 1955, if we ignore the peak in 1960 that was caused by image quality; this is the same period during which grass cover decreased dramatically. Similar observations have been recorded on the adjacent Jornada Experimental Range, where transect data from a 259-ha enclosure showed that black grama had a 71% frequency in 1935, and decreased sharply between 1950 and 1955 from 56% to 9% frequency. In that same area, mesquite canopy frequency doubled between 1935 and 1980, with over half of this increase occurring between 1935 and 1950 (Hennessy et al., 1983). In another study of permanent 1-$m^2$ quadrats, it was shown that perennial grass basal area was positively associated with the precipitation of

Table 3
Precipitation data (in mm) for six rain gauges within a 6-km radius of the study area for September 1996 compared to long-term average (1937–2003) for September

| Rain gauge | September 1996 | Long-term average for September |
|---|---|---|
| Camp well | 63.5 | 36.8 |
| Selden well | 46.2 | 34.8 |
| Headquarters | 68.1 | 34.3 |
| Parker heights | 65.3 | 34.8 |
| V.M. playa | 50.6 | 29.2 |
| P 3 south | 53.1 | 32.0 |

the previous 3–4 years and that drought had a strong influence on black grama (Gibbens & Beck, 1988). Precipitation data from 1937 to 2003 are shown in Fig. 8. The stages and thresholds of this desertification process have been described recently by Peters et al. (in press).

The severe drought that occurred in 1951–1956 was one of the major factors in this vegetation change (Buffington & Herbel, 1965), leading to a decrease in black grama, which was followed by the spread of mesquite into areas previously occupied by black grama. The mesquite is more successful during dry periods because unlike grasses, shrubs can take advantage of moisture located deeper in the soil profile. This vegetation change alters site conditions, favoring the formation of mesquite dunes and altering soil water regimes, which in turn makes it difficult for black grama to become established again, even if moisture conditions become favorable for grasses (Archer, 1995; Hennessy et al., 1983). Unfortunately, we lack additional image data during the drought period to document those vegetation changes in more detail. The increase in shrub cover from 1991 to 2003 may be related to the general decline in precipitation since 1992. Although an increase in precipitation was observed from 1994 to 2000, precipitation levels after 2000 have been nearly as low as they were in the 1951–1956 drought.

Shrub cover was variable in some years. This variation may be an artifact of different image quality or a biological reality. We observed a decline in shrub cover after the January 1973 image was taken. This may be attributed to herbicide spraying in pasture 2 in June 1973. The effects were observed on the 1977 aerial photo where a linear pattern was visible in the southern part of the study area. This effect can also be seen on the shrub classification maps (Fig. 3), where this pattern is first visible in 1989, then becomes more defined from 1991 through 2003. In the 2003 QuickBird image, the pattern is especially noticeable.

Another pattern visible on the shrub classification maps are lines of dense shrubs running from the southwest to the northeast; those lines are old cattle trails. Cattle are very effective at dispersing mesquite seeds because they consume mesquite beans, and seeds remain viable after passage. In fact, passage through the digestive tract may increase seed germination two- to threefold (Brown & Archer, 1987). Once plants are established, they facilitate the recruitment of new plants (Archer, 1995). The lines of dense shrubs appear to get fainter over time; however, close-up investigation showed that shrubs did not disappear over time, but that other shrubs filled in around the original plants, making the lines appear less distinct. The trails were probably established during a time of heavier grazing pressure, which occurred in pasture 2 from 1936 to 1953 (7.2 AUD/ha (animal unit days)). From 1954 to 1963, grazing was reduced to 0.9 AUD/ha. Around this time, grazing was also changed from year round to summer into early fall grazing at 4.8 AUD/ha during the 1970s and 1980s. In the 1990s, fences were moved and grazing has been minimal due to lack of permanent water source. However, the old trails remain visible due to the denser growth of mesquite shrubs.

Broad-scale patterns on the landscape such as cattle trails and evidence of herbicide spraying are often detected only with remotely sensed imagery and may be difficult or impossible to discern on the ground. Therefore, remote sensing is a valuable tool for tracking such patterns over time or determining past treatments that may not have been recorded elsewhere (Goslee et al., 2003; Rango & Havstad, 2003; Rango et al., 2002).

Shrubs increased in this study area from 1937 to 2003 regardless of whether they were located in the grass, bright soil, or others classes (Fig. 6). However, shrub cover within the grass class was higher after 1955 until 1989. This is in agreement with the theory that the 1951–1956 drought was a major factor in vegetation change. Grasses (especially black grama) decreased during the drought, which allowed the shrub cover to increase in areas occupied by grasses. After 1989, shrub cover increased in all classes, presumably because of a general decline in precipitation. The playa had denser shrub cover than the other classes until 1967, when a sudden drop in shrub cover occurred. This was attributed to a mechanical shrub removal in the playa between 1967 and 1973 in order to improve livestock watering facilities.

The correlation between ground-based shrub measurements and estimates from image classification depends on the size of shrubs and image resolution (Ansley et al., 2001; Goslee et al., 2003). Our images contained many small shrubs and only 29% of shrubs smaller than 2 $m^2$ were

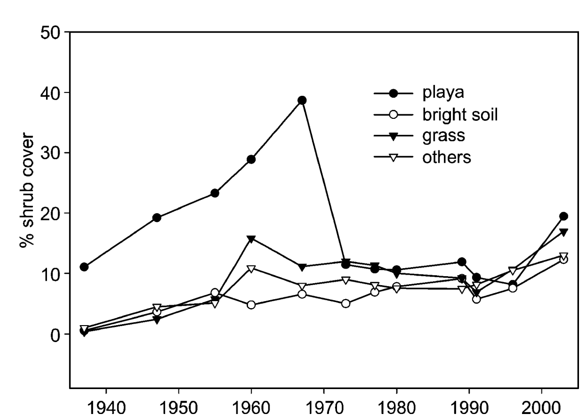


Fig. 6. Percent shrub cover in four classes of the level 2 classification shown in Fig. 4.

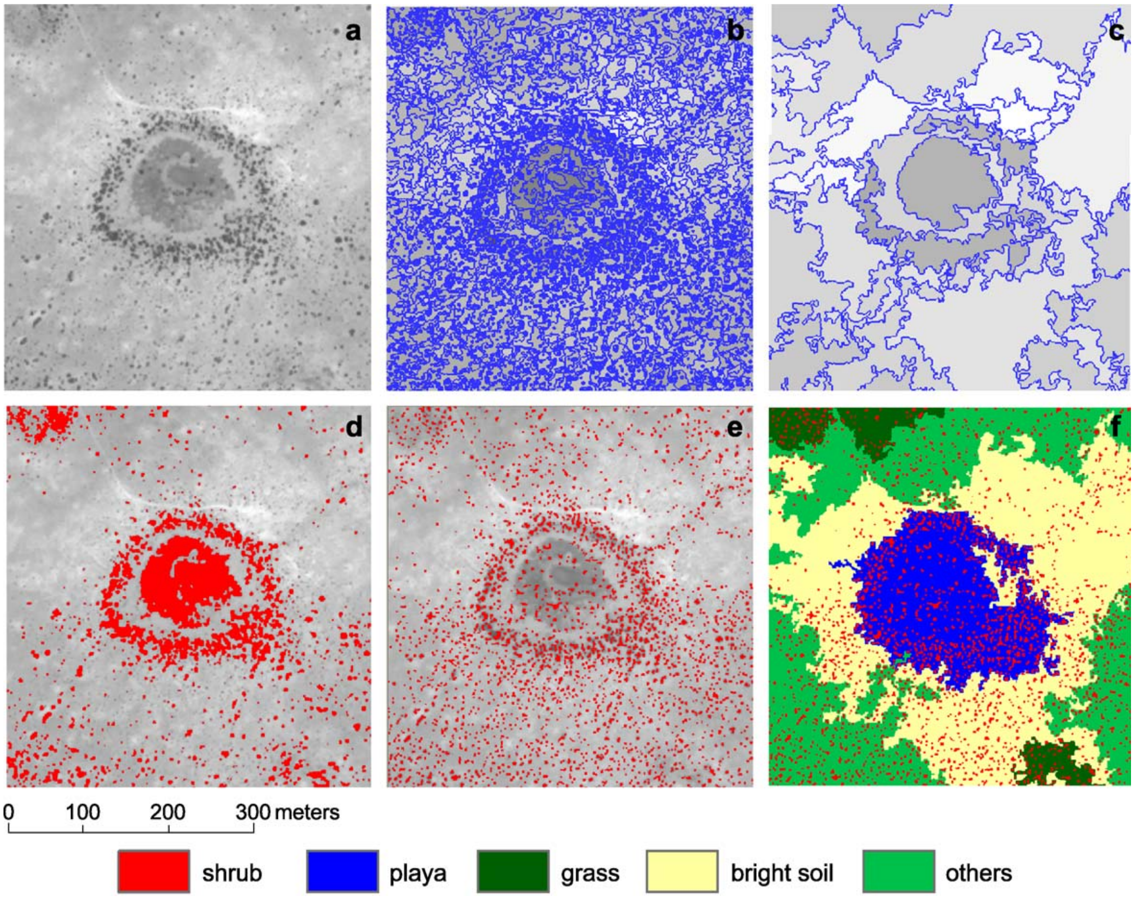


Fig. 7. Steps in the segmentation and object-based analysis of the images. (a) Portion of original QuickBird image, (b) segmentation at level 1 of the image object hierarchy, (c) segmentation at level 2, (d) classification using only the mean spectral reflectance of the segmented objects results in overestimation of shrub cover, (e) linkage between neighboring objects and level 2 objects results in improved classification of shrub cover, and (f) classification-based segmentation results in merged classification of both levels.

detected, resulting in an underestimation of shrub cover from the classification. Although visual assessment showed a very good correlation between the shrub outlines from GPS compared to the classification, we have to accept an inherent error associated with measuring relatively small shrubs with a moving GPS unit.

In order to assess how closely our grass classification resembled actual conditions in the 1930s, we located early survey information. In a 1935–1938 vegetation survey, only 2% of the area was dominated by mesquite, while the rest was dominated by grass: 63% of the area was occupied by dropseed, 34% by black grama, and 1% by tobosa. It is somewhat difficult to compare our classification from aerial photography with the vegetation survey map. Those surveys produced quite broad boundaries for vegetation, lacking the detail that can be seen from aerial photos. On the other hand, the dropseed genera are more difficult to detect from aerial photos compared to black grama or tobosa because these latter species have a more distinct reflectance. For this study, we did not try to distinguish between black grama and tobosa because both appeared similar in panchromatic aerial photos. The vegetation surveys from 1935 to 1938 did not mention mesquite as a second or third dominant species in the dropseed or black grama class; therefore, we assumed that areas we classified as “others” in 1937 were in fact predominantly grasslands, although we detected some shrubs in them.

Table 4
Statistics from ground truth data for shrubs that were detected and not detected with the image classification

| | All shrubs | Detected | Not detected |
|---|---|---|---|
| Count | 270 | 180 | 90 |
| Mean area ($m^2$) | 6.12 | 8.39 | 1.58 |
| Standard error | 0.55 | 0.77 | 0.12 |
| Minimum | 0.28 | 0.31 | 0.28 |
| Maximum | 75.13 | 75.13 | 6.90 |

The difficulties we encountered related to varying image qualities of the aerial photos. Unfortunately, we had little metadata on film and camera type for the aerial photography. Spatial and spectral resolution, contrast, and sun angle were highly variable for the set of images used. Although all images were resampled to a common spatial resolution, differences in quality were still evident. A case in point was the 1960 image, in which shrubs tended to blur together, making them appear larger than in the other

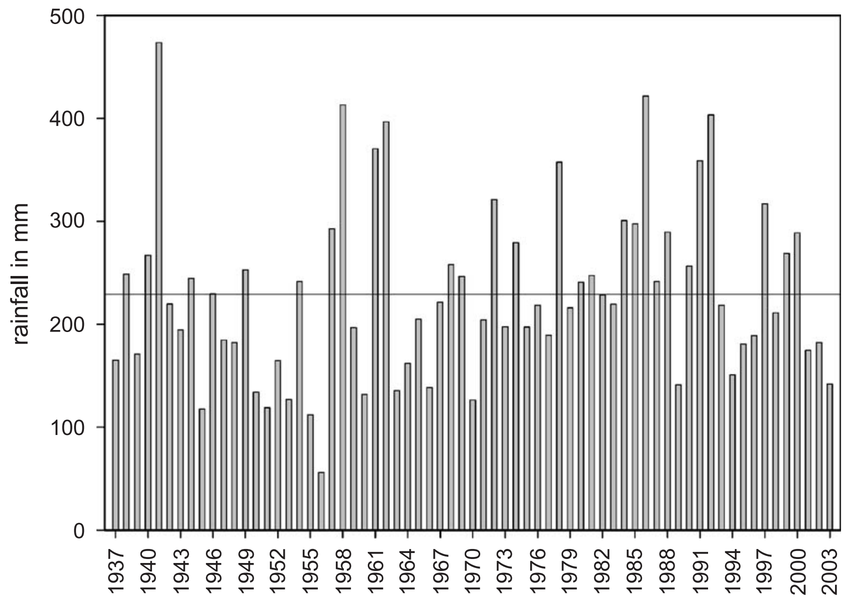


Fig. 8. Mean annual precipitation at Selden Well rain gauge, located 2.5 km from study area. Horizontal line indicates mean rainfall.

images. This led to a probable overestimation of shrub cover for that year.

Another difficulty lay in separating image quality from ecological variations because the images were taken at different times of the year. Moisture conditions vary not only over long periods but precipitation patterns are also highly variable from one year to the next in this region. In addition, grasses are able to respond relatively quickly to a rain event, which was evident in the October 1996 image, which showed a peak in grass cover due to high precipitation in September. Some suffrutescents, such as broom snakeweed, can also respond to rain and may be confused with black grama. For a series of images ranging from 1937 to 2003, all taken at different times of the year and with varying qualities, one important indicator of change is the general trend of vegetation cover over time. Peaks and troughs in the vegetation cover are often related to precipitation events, but effects due to image quality have to be taken into consideration.

Although we performed the same analysis on both the aerial photos and the satellite image, some differences between the imagery have to be kept in mind. The fact that a larger proportion of small shrubs were captured with the QuickBird image is associated with the different bit depth in the QuickBird image compared to the aerial photos. With aerial photography, data are placed into 256 levels (8 bits of data in a binary encoding system). The bands of the QuickBird sensor are placed into 2048 levels (11 bits), giving the latter a higher radiometric resolution which allows for a greater grey-scale range. In addition, poor quality and lack of contrast in some of the aerial photography prevented the capturing of many small shrubs.

This analysis compared only classified shrubs with those measured on the ground. However, we noticed that many shrubs measured with GPS could actually be seen on the QuickBird images, but were not captured with the object-based classification. One reason for this is that we only used the panchromatic band of the QuickBird image and it was degraded from the original 61-cm resolution to 86 cm. It is possible that more shrubs can be captured with QuickBird images by exploiting the original pixel size and multi-spectral information in a pan-sharpened image. Another reason is related to the values in the membership functions. Further fine tuning of the values chosen for mean brightness, mean difference to neighbors and mean difference to super-object may increase the number of shrubs captured by including brighter objects (shrubs) without including relatively similar brighter backgrounds (soil surfaces).

The object-based classification techniques used in this study proved a valuable tool for detecting vegetation change over time and were especially applicable to the detection of shrubs. Objects of similar spectral reflectance as shrubs could be omitted by describing differences between neighboring objects as well as objects on a different hierarchical level. In addition, the linking of levels allowed for the analysis of shrub densities in higher level classes. Although the segmentation algorithm used here performed well with our images, it would be worthwhile to investigate if other multifractal segmentation techniques (Chaudhuri & Sarkar, 1995; Vehel & Mignot, 1994) could improve class boundaries.

Future studies will examine alternative approaches to analyzing images of different resolutions. Rather than resampling all images to the same pixel size, an alternate approach would be to use object-specific analysis and upscaling (Hay et al., 2001), where spatial measures specific to the image are used in a weighting function to resample or upscale an image to a coarser resolution. Related techniques are described by Woodcock and Strahler (1987) and Marceau et al. (1994).

## 5. Conclusions

In this study, we assessed the rate of shrub encroachment into a desert grassland using remotely sensed imagery. Although shrub increase in the Jornada Basin has been well documented using plot level data, imagery covers larger areas and can give insights into overall spatial and temporal patterns. In this study area, shrub cover increased and grass cover decreased over time, but these changes were nonlinear. The vegetation dynamics reflected influences from livestock due to mesquite establishment along cattle trails as well as broad- and fine-scale changes in precipitation patterns. At a fine scale, a peak in grass cover was observed in an image taken after a particularly wet month (September 1996). During and following the 1951–1956 drought, shrub cover increased and grass cover decreased at a greater rate than in the following years, except for 1991–2003. The increase in recent years was attributed in part to a general decline in precipitation since 1992 and the higher radiometric resolution of the QuickBird image.

Although the trends in the vegetation dynamics followed those of long-term plot data recorded over time, the image analysis tended to underestimate shrub cover due to a lower level of detail in the classification compared to GPS ground truth data. Nevertheless, 87% of shrubs larger than 2 $m^2$ were detected with the classification. The object-oriented multiscale image analysis method used here has several advantages over a pixel-based classification approach when the goal is the extraction of relatively small objects such as shrubs from panchromatic aerial photos and high-resolution satellite images. This method approximates the way humans interpret information visually from aerial photos, but has the advantage of an automated classification routine. In a traditional pixel-based classification, it would prove difficult to classify small shrubs and larger land cover areas in the same step without getting a significant "salt and pepper effect". Image segmentation at multiple resolutions allowed for analysis at the shrub level and for grasses at a coarser level with a subsequent merging of both classifications. With a hierarchical image analysis, the same image is classified at different scales. Classified objects on one scale are kept separate from those on another scale, but can be merged by applying expert knowledge, a method that is appropriate in an ecological sense.

Using aerial photos in automated image analysis brings with it many challenges, including differences in contrast, spectral and spatial resolutions, sun angle and time of day/year of acquisition. Nevertheless, historical photos in conjunction with plot-based records and appropriate ground truth information provide an important record of vegetation dynamics over time. The techniques described here show promise for quantifying shrub encroachment using aerial and high-resolution satellite imagery over larger areas, so that proper management practices can be applied at the proper times to these sites.

## Acknowledgments

This research was funded by the USDA Agricultural Research Service and the National Science Foundation Long-Term Ecological Research Program, Jornada Basin IV: Linkages in Semiarid Landscapes.

## References

Abkar, A. A., Sharifi, M., & Mulder, N. (2000). Likelihood-based image segmentation and classification: A framework for the integration of expert knowledge in image classification procedures. *International Journal of Applied Earth Observation and Geoinformation*, *2*(2), 101–119.

Ansley, R. J., Wu, X. B., & Kramp, B. A. (2001). Observation: Long-term increases in mesquite canopy cover in a North Texas savanna. *Journal of Range Management*, *54*(2), 171–176.

Archer, S. (1994). Woody plant encroachment into southwestern grasslands and savannas: Rates, patterns and proximate causes. In M. Vavra, W. A. Laycock, & R. D. Pieper (Eds.), *Ecological implications of livestock herbivory in the West* (pp. 13–68). Denver, CO: Society for Range Management.

Archer, S. (1995). Tree-grass dynamics in a Prosopis–thornscrub savanna parkland: Reconstructing the past and predicting the future. *Ecoscience*, *2*(1), 83–99.

Baatz, M., & Schaepe, A. (2000). Multiresolution segmentation: an optimization approach for high quality multi-scale image segmentation. In J. Strobl, & T. Blaschke (Eds.), *Angewandte geographische informationsverarbeitung*, *vol. XII*. (pp. 12–23). Heidelberg, Germany: Wichmann.

Blaschke, T., & Hay, G. J. (2001). Object oriented image analysis and scale-space: Theory and methods for modeling and evaluating multiscale landscape structure. *International Archives of Photogrammetry and Remote Sensing*, *34*(4), 22–29.

Blaschke, T., & Strobl, J. (2001). What's wrong with pixels? Some recent developments interfacing remote sensing and GIS. *GeoBIT/GIS*, *6*, 12–17.

Benz, U. C., Hoffmann, P., Willhauck, G., Lingenfelder, I., & Heynen, M. (2004). Multi-resolution, object-oriented fuzzy analysis of remote sensing data for GIS-ready information. *ISPRS Journal of Photogrammetry and Remote Sensing*, *58*, 239–258.

Brown, J. R., & Archer, S. (1987). Woody plant seed dispersal and gap formation in a North American subtropical savanna woodland: The role of domestic herbivores. *Vegetatio*, *73*, 73–80.

Brown, J. R., & Carter, J. (1998). Spatial and temporal patterns of exotic shrub invasion in an Australian tropical grassland. *Landscape Ecology*, *13*, 93–102.

Buffington, L. C., & Herbel, C. H. (1965). Vegetational changes on a semidesert grassland range from 1858 to 1963. *Ecological Monographs*, *35*(2), 139–164.

Burnett, C., & Blaschke, T. (2003). A multi-scale segmentation/object relationship modelling methodology for landscape analysis. *Ecological Modelling*, *168*(3), 233–249.

Chaudhuri, B. B., & Sarkar, N. (1995). Texture segmentation using fractal dimension. *Pattern Machine and Intelligence*, *17*(1), 72–77.

Definiens (2003). "Definiens Imaging, eCognition." Web page, [accessed 7 October 2003]. Available at http://www.definiens-imaging.com

Franklin, S. E., Hall, R. J., Moskal, L. M., Maudie, A. J., & Lavigne, M. B. (2000). Incorporating texture into classification of forest species composition from airborne multispectral images. *International Journal of Remote Sensing*, *21*(1), 61–79.

Gibbens, R. P., & Beck, R. F. (1988). Changes in grass basal area and forb densities over a 64-year period on grassland types of the Jornada Experimental Range. *Journal of Range Management*, *41*(3), 186–192.

Gibbens, R. P., McNeely, R. P., Havstad, K. M., Beck, R. F., & Nolen, B. (In press). Vegetation changes in the Jornada Basin from 1858 to 1998. *Journal of Arid Environments.*

Goslee, S. C., Havstad, K. M., Peters, D. P. C., Rango, A., & Schlesinger, W. H. (2003). High-resolution images reveal rate and pattern of shrub encroachment over six decades in New Mexico, U.S.A. *Journal of Arid Environments*, *54*, 755–767.

Grover, H. D., & Musick, B. (1990). Shrubland encroachment in southern New Mexico, USA: An analysis of desertification processes in the American southwest. *Climatic Change*, *17*, 305–330.

Haddon, J. F., & Boyce, J. F. (1990). Image segmentation by unifying region and boundary information. *IEEE Transactions on Pattern Analysis and Machine Intelligence*, *12*(10), 929–948.

Hansen, D. J., & Ostler, W. K. (2001). An evaluation of new high-resolution image collection and processing techniques for estimating shrub cover and detecting landscape changes. *Proceedings of the 18th Biennial Workshop on Color Photography and Videography in Resource Assessment*. Bethesda, MD: American Society for Photogrammetry and Remote Sensing.

Haralick, R. M., & Shapiro, L. G. (1985). Image segmentation techniques. *Computer Vision, Graphics and Image Processing*, *29*, 100–132.

Haralick, R., Shanmugan, K., & Dinstein, I. (1973). Textural features for image classification. *IEEE Transactions on Systems, Man and Cybernetics*, *3*(1), 610–621.

Havstad, K. M., Kustas, W. P., Rango, A., Ritchie, J. C., & Schmugge, T. J. (2000). Jornada experimental range: a unique arid land location for experiments to validate satellite systems. *Remote Sensing of Environment*, *74*, 13–25.

Hay, G. J., Dube, P., Bouchard, A., & Marceau, D. J. (2002). A scale-space primer for exploring and quantifying complex landscapes. *Ecological Modelling*, *153*, 27–49.

Hay, G. J., Marceau, D. J., Dube, P., & Bouchard, A. (2001). A multiscale framework for landscape analysis: Object-specific analysis and upscaling. *Landscape Ecology*, *16*, 471–490.

Hennessy, J. T., Gibbens, R. P., Tromble, J. M., & Cardenas, M. (1983). Vegetation changes from 1935 to 1980 in mesquite dunelands and former grasslands of southern New Mexico. *Journal of Range Management*, *36*(3), 370–374.

Herold, M., Liu, X., & Clarke, K. C. (2003). Spatial metrics and image texture for mapping urban land use. *Photogrammetric Engineering and Remote Sensing*, *69*(9), 991–1001.

Hudak, A. T., & Wessman, C. A. (1998). Textural analysis of historical aerial photography to characterize woody plant encroachment in South African savanna. *Remote Sensing of Environment*, *66*, 317–330.

Lillesand, T. M., & Kiefer, R. W. (2000). *Remote sensing and image interpretation*. (4th ed.) New York: Wiley.

Marceau, D. J., Howarth, P. J., & Gratton, D. J. (1994). Remote sensing and the measurement of geographical entities in a forested environment: 1. The scale and spatial aggregation problem. *Remote Sensing of Environment*, *49*, 93–104.

McCloy, K. R., & Hall, K. A. (1991). Mapping the density of woody vegetation cover using Landsat MSS digital data. *International Journal of Remote Sensing*, *12*(9), 1877–1885.

Peters, D. P. C., Pielke, R. A., Bestelmeyer, B. T., Allen, C. D., Munson-McGee, S., & Havstad, K. M. (In press). Spatial nonlinearities: Cascading effects in the earth system. *Science*.

Rango, A., & Havstad, K. M. (2003). The utility of historical aerial photographs for detecting and judging the effectiveness of rangeland remediation techniques. *Environmental Practice*, *5*(2), 107–118.

Rango, A., Goslee, S., Herrick, J., Chopping, M., Havstad, K. M., Huenneke, L., et al. (2002). Remote sensing documentation of historic rangeland remediation treatments in southern New Mexico. *Journal of Arid Environments*, *50*, 549–572.

Reed, T. R., & Wechsler, H. (1990). Segmentation of textured images and gestalt organization using spatial/spatial frequency representations. *IEEE Transactions on Pattern Analysis and Machine Intelligence*, *12*, 1–12.

Ryherd, S., & Woodcock, C. E. (1996). Combining spectral and texture data in the segmentation of remotely sensed images. *Photogrammetric Engineering and Remote Sensing*, *62*(2), 181–194.

Schlesinger, W. H., Reynolds, J. F., Cunningham, G. L., Huenneke, L. F., Jarrell, W. M., Virginia, R. A., et al. (1990). Biological feedbacks in global desertification. *Science*, *247*, 1043–1048.

Thomas, N., Hendrix, C., & Congalton, R. G. (2003). A comparison of urban mapping methods using high-resolution digital imagery. *Photogrammetric Engineering and Remote Sensing*, *69*(9), 963–972.

Turner, M. G., & Gardner, R. H. (1994). Quantitative methods in landscape ecology. New York: Springer-Verlag.

Vehel, J., & Mignot, P. (1994). Multifractal segmentation of images. *Fractals*, *2*(3), 371–378.

Whiteman, G., & Brown, J. R. (1998). Assessment of a method for mapping woody plant density in a grassland matrix. *Journal of Arid Environments*, *38*, 269–282.

Woodcock, C. E., & Strahler, A. H. (1987). The factor of scale in remote sensing. *Remote Sensing of Environment*, *21*, 311–332.